ELSEVIER

Materials Science and Engineering A214 (1996) 146–152

MATERIALS SCIENCE & ENGINEERING A

Mechanism of mechanical alloying in Ni–Al and Cu–Zn systems

S.K. Pabi, B.S. Murty

Department of Metallurgical and Materials Engineering, Indian Institute of Technology, Kharagpur 721302, India

Received 1 August 1995; revised 12 February 1996

Abstract

Nanocrystalline Al_3Ni, NiAl and Ni_3Al phases in the Ni–Al system and the α, β, γ and ϵ phases in the Cu–Zn system were synthesized by mechanical alloying of elemental blends in a planetary mill. In the as-milled state, Al_3Ni and AlNi were always ordered, while Ni_3Al was disordered. MA results in a large extension of the NiAl and Ni_3Al phase fields particularly towards Al-rich compositions. The crystallite size was finest (~ 6 nm) when NiAl and Ni_3Al phases coexist after prolonged milling. In contrast, in all Cu–Zn blends containing 15–85 at.% Zn, the Zn-rich phases were first to form and final crystallite sizes were coarser (15–80 nm). Two different modes of alloying have been identified. In the case of NiAl and Al_3Ni, where the ball milled product is ordered and the heat of formation is large ($\Delta H_f > 120$ kJ mol^{-1}), a rapid discontinuous mode of alloying accompanied with an additive increase in crystallite size is detected. In all other cases irrespective of the magnitude of ΔH_f, gradual diffusive mode of intermixing during milling seems to be the underlying mechanism of alloying.

Keywords: Mechanical alloying; Nanocrystals; Milling

1. Introduction

The pioneering work of Benjamin [1], has led to the evolution of mechanical alloying (MA) as a solid state processing route which cannot only produce equilibrium phases but also nonequilibrium phases such as amorphous phases [2–5]. Synthesis of intermetallic and other compounds by mechanical alloying (MA) of elemental blends has been the subject of interest to many investigators in recent years [2,6–14]. Most of these investigations report the formation of one or more compounds in nanocrystalline form. However, reports on the mechanism of alloying during ball milling are relatively few in number [9,15]. By in situ measurement of vial temperature during MA in a SPEX mill, Atzmon [9] found that NiAl forms in equiatomic mixture of Ni and Al through an explosive exothermic reaction, similar to the self-propagating high temperature synthesis reaction [16]. Zbiral et al. [15] have suggested that alloying, in general, occurs by the diffusion of either one element or both the elements depending on the equilibrium solid solubility. In an A–B system with significant solubility of B in A and relatively insolubility of A in B, alloying occurs by the diffusion of B into A. In cases where the mutual solid solubility is appreciable, alloying seems to take place by the diffusion of both elements into each other. It is, however, not clear under what conditions such a diffusion model is applicable to the formation of compounds by MA. The present paper reports a systematic study of the mechanism of mixing in two model systems, namely, Ni–Al and Cu–Zn, that have widely different heats of formation (ΔH_f). The equilibrium diagrams of both the systems show the presence of terminal solid solutions and intermetallic compounds [17]. In Ni–Al system, the intermetallic compounds such as NiAl, Ni_3Al or Al_3Ni have large ΔH_f of > 120 kJ mol^{-1} [18]. Moreover, NiAl is known to remain ordered up to its melting point, while Ni_3Al seems to have a relatively low ordering energy (5 kJ mol^{-1}) and low disordering temperature (638 K) [19,20]. In contrast, the intermetallic phases in the Cu–Zn system are electron compounds with low ΔH_f (~ 8 kJ mol^{-1}) [21].

2. Experimental

High purity Ni and Al (99.9%) powders were mixed in the proportions of $Al_{100-x}Ni_x$ ($x = 10$, 18, 21, 25, 40, 50, 65, 68, 70, 75 and 90) and were mechanically alloyed in a FRITSCH Pulverisette-5 planetary mill. The milling was carried out at 300 rpm in WC con-

0921-5093/96/$15.00 © 1996 — Elsevier Science S.A. All rights reserved

tainer in toluene using 10 mm diameter WC balls with ball to powder weight ratio of 10:1. Similarly, elemental blends of Cu (99.9%) and Zn (99.5%) of compositions $Cu_{100-x}Zn_x$ ($x = 15$, 30, 40, 50, 65 and 85) were mechanically alloyed in a steel container using 10 mm diameter steel balls. The mechanically alloyed powders were characterised by a Philips PW 1840 X-ray diffractometer with CuKα radiation at regular intervals of milling. The crystallite size was calculated from X-ray diffraction (XRD) peak broadening after separation of the contributions of strain and instrumental broadening by standard procedure [22]. The crystallite size was confirmed by transmission electron microscopy (TEM) using Philips CM12.

3. Results

3.1. Synthesis of Ni aluminides by MA

Nanocrystalline Al_3Ni, NiAl and Ni_3Al have been synthesized by MA in the present study. MA of elemental blend of $Al_{90}Ni_{10}$ composition has not resulted in the formation of any aluminide and the peaks of Al and Ni persisted in the XRD pattern even after 30 h of milling. In contrast, $Al_{82}Ni_{18}$ and $Al_{79}Ni_{21}$ have shown the formation of Al_3Ni. Fig. 1 shows the evolution of Al_3Ni in $Al_{79}Ni_{21}$ composition during MA. Here, the residual Al present after 20 h of milling completely disappeared on further milling up to 30 h. Some residual Al, however, persisted in the case of $Al_{82}Ni_{18}$ even after 30 h of MA. The superlattice reflections of Al_3Ni indicated by arrow-heads evidence that the Al_3Ni generated by MA remains ordered in the as milled condition. No notable shift of the XRD peaks of Al in these alloys suggests that ball milling is not effective in extending the solid solubility of Ni in Al.

Contrary to the expectations, MA of Al and Ni in stoichiometric ratio of Al_3Ni, i.e. $Al_{75}Ni_{25}$ blend has shown that Al_3Ni formed along with NiAl in the early stages (12 h) of milling disappears on further milling up to 20 h, leaving behind NiAl, as has already been

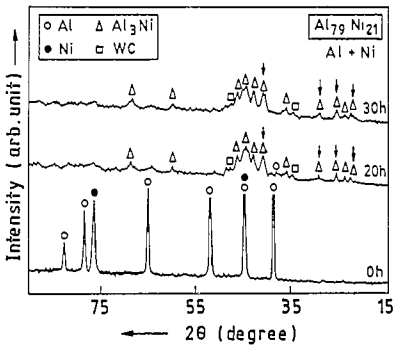

Fig. 1. XRD patterns of $Al_{79}Ni_{21}$ blend as a function of milling time showing the evolution of Al_3Ni.

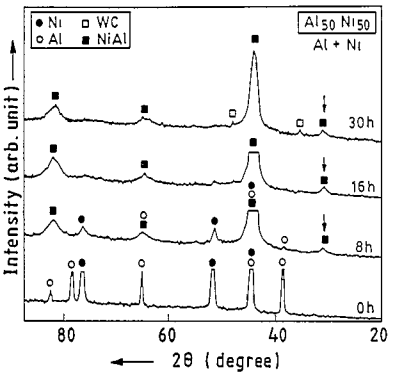

Fig. 2. XRD patterns of $Ni_{50}Al_{50}$ blend at different milling time showing NiAl formation.

reported earlier [14]. Single phase NiAl was also found to be the end product of milling for $Al_{60}Ni_{40}$ and $Al_{50}Ni_{50}$ compositions. Fig. 2 illustrates the time modulation of XRD patterns in course of milling $Al_{50}Ni_{50}$ elemental blend Here the formation of NiAl can be noticed within 8 h of MA. Further milling up to 16 h resulted in the disappearance of XRD peak for Al, while the Ni peaks persisted up to 20 h. The NiAl produced in all the compositions was ordered as manifested by the superlattice reflections (e.g. see arrowhead in Fig. 2). The nanocrystalline nature of the NiAl synthesized in the present study can be clearly seen from the TEM bright field image in Fig. 3. The average size of the particles was about 10 nm. The selected area electron diffraction pattern from these particles (inset of Fig. 3) confirms the absence of any amorphous phase.

MA of $Al_{35}Ni_{65}$ and $Al_{32}Ni_{68}$ has shown a two-phase mixture of ordered NiAl and disordered Ni_3Al. MA of Ni-rich compositions (70–90 at.% Ni) has yielded single phase disordered Ni_3Al. The evolution of disordered Ni_3Al during MA is clearly evident from Fig. 4. No

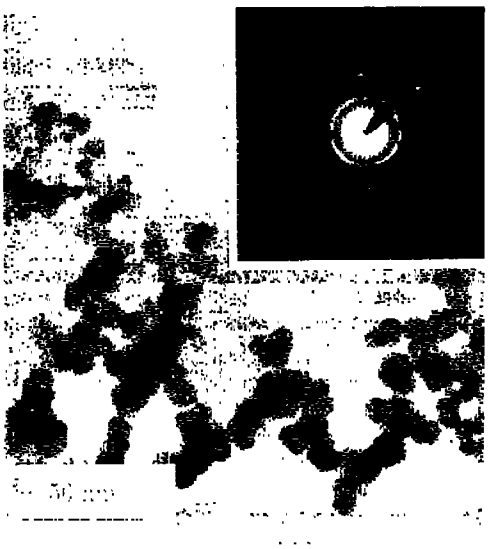

Fig. 3. TEM bright field image of nanocrystalline NiAl. Inset shows the selected area diffraction pattern from NiAl.

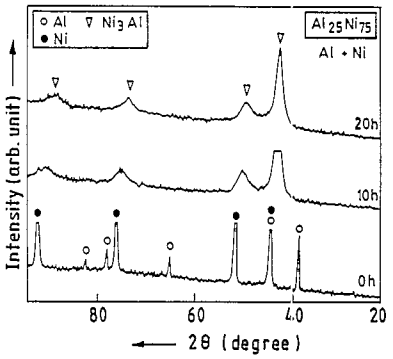

Fig. 4. XRD patterns of $Al_{25}Ni_{75}$ at different milling intervals depicting the formation of disordered Ni_3Al.

XRD peak shifts were observed for Al, while Ni peaks shifted continuously towards the Ni_3Al peak positions with increase in milling time. Within 20 h of milling, the peak positions matched closely with the fundamental lines of Ni_3Al and no peak shifts were observed with further milling. As the peak positions of the phase formed matched perfectly with the fundamental reflections of Ni_3Al, at all the Ni-rich compositions studied (i.e., 70, 75 and 90 at.% Ni), the phase formed is referred to as disordered Ni_3Al rather than solid solution of Al in Ni, i.e., Ni(Al).

Fig. 5 compares the phase field extensions obtained by MA for the aluminides with their equilibrium phase fields. It is interesting to note that while Al_3Ni is a line compound under equilibrium conditions, MA could result in its formation at compositions away from its stoichiometry. In ball milled product, NiAl phase field manifests a large extension from 25 to 65 at.% Ni (equilibrium range is 45 to 58 at.% Ni). Similarly

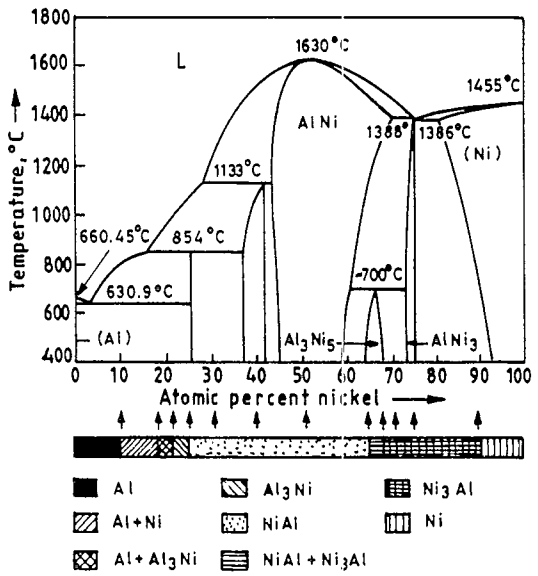

Fig. 5. The phase fields of different aluminides observed after 30 h of MA in relation to the equilibrium phase fields indicated by the phase diagram.

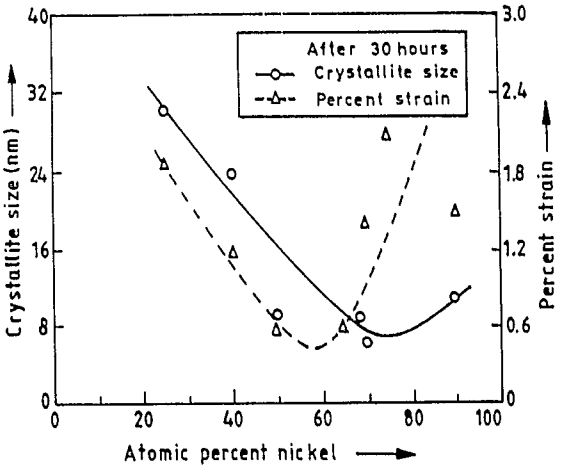

Fig. 6. Variation of crystallite size and strain with composition in the Ni–Al system after MA for 30 h.

disordered Ni_3Al phase field has also been extended from 70 to 90 at.% Ni as against the narrow equilibrium range of 74 to 76 at.% Ni for ordered Ni_3Al.

The crystallite sizes and lattice strain after prolong milling ($\sim$30 h) of different alloy compositions are shown in Fig. 6. It is interesting to note that crystallite size reaches a minimum ($\sim$6 nm) at compositions where a two phase mixture of NiAl and Ni_3Al coexists. The r.m.s. strain appear to reach its minimum value near this range, possibly due to the ease of stress relaxation in smaller crystallite sizes. TEM study has confirmed that the crystallite size of Al_3Ni is larger than that of NiAl (Figs. 7 and 3) and the observed sizes are in good agreement with the values estimated from XRD data.

3.2. Mixing phenomenon

3.2.1. Ni–Al system

Observation of XRD patterns of different compositions in this system has shown that ordered AL_3Ni and

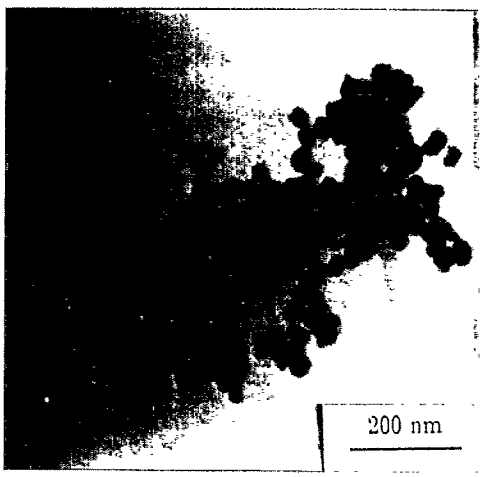

Fig. 7. TEM bright field image showing the nanocrystalline nature of Al_3Ni.

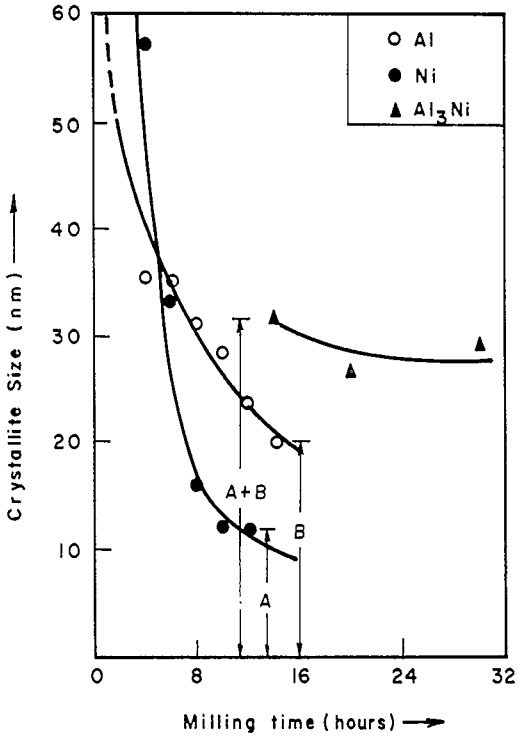

Fig. 8. Variation of crystallite size of constituent metals with milling time during the formation of Al_3Ni in $Al_{79}Ni_{21}$ blend.

NiAl form all of a sudden while disordered Ni_3Al forms by continuous shifts in ni peaks. Study of the crystallite sizes has evidenced the NiAl or Al_3ni formation is triggered only when Al and Ni reach critical nanocrystalline sizes. In both cases it was observed that the crystallite sizes of Al_3Ni and NiAl at the time of their formation were equal to the sum of the crystallite sizes of their constituents (Al and Ni) as shown in Figs. 8 and 9. The critical crystallite sizes of Ni and Al required for the onset of NiAl formation in $Ni_{50}Al_{50}$ composition are found to be larger than that in $Ni_{25}AlL_{75}$.

3.2.2. Cu–Zn system

The sequence of phase transformation in six nominal compositions of this system is summarised in Table 1. It

Table 1
Transformation sequence during MA of different Cu–Zn blends

Composition	Transformation Sequence
$Cu_{85}Zn_{15}$	$\epsilon \rightarrow \alpha + ZnO$
$Cu_{70}Zn_{30}$	$\epsilon + \gamma \rightarrow \beta \rightarrow \alpha + ZnO$
$Cu_{60}Zn_{40}$	$\epsilon + \gamma \rightarrow \beta + \alpha \rightarrow \alpha + ZnO$
$Cu_{50}Zn_{50}$	$\epsilon + \gamma \rightarrow \epsilon + \gamma + \beta \rightarrow \beta + M \rightarrow \beta + \alpha + ZnO \rightarrow \alpha + ZnO$
$Cu_{35}Zn_{65}$	$\epsilon + \gamma \rightarrow \gamma \rightarrow \gamma + \beta + ZnO \rightarrow \beta + ZnO$
$Cu_{15}Zn_{85}$	$\epsilon \rightarrow \epsilon + ZnO \rightarrow \epsilon + \gamma + ZnO$

M refers to martensite.

is apparent that irrespective of the blend composition, Zn-rich ϵ and γ phases are first to form in the early stages of MA (Fig. 10). Further milling lead to the generation of stable phases that almost conform to the equilibrium phase fields. Rapid diffusion of Zn into Cu and formation of α phase was observed only after Cu crystallites reach almost 15 nm size (Fig. 11). The marginal decrease in the Zn content in α after prolonged milling was associated with ZnO formation. The results in the Cu–Zn system indicate that for compositions < 50 at.% Zn, the Cu-rich phases have formed by direct destabilisation of Zn-rich phases owing to diffusion of Cu, while in blends containing > 50 at.% Zn, the Cu rich phases seem to form owing to the loss of Zn in Zn-rich phases by oxidation. The pattern of XRD peak shift and crystallite size measurements reveal that the phases in Cu–Zn system form by diffusion of Cu and Zn in each other in course of milling in a manner similar to the mechanism of formation of disorderd Ni_3Al. The only difference in these two cases is that in Cu–Zn system, diffusion of both Cu and Zn in each other was responsible for the formation of different phases, while the formation of disordered Ni_3Al was caused by the diffusion of Al alone into Ni.

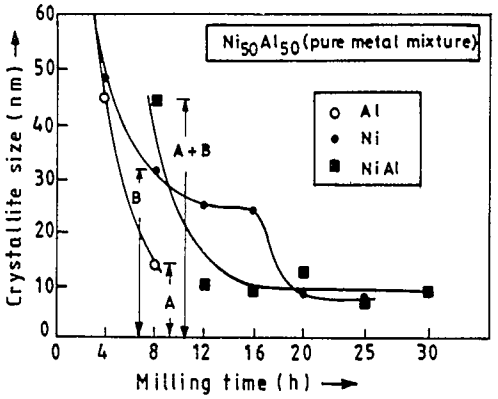

Fig. 9. Crystallite sizes of defferent phases during MA of $Al_{75}Ni_{25}$ composition as a function of milling time.

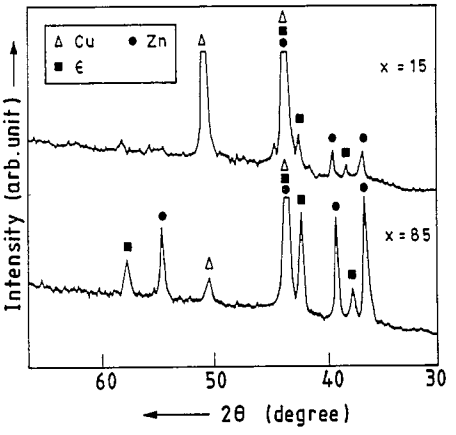

Fig. 10. XRD patterns of $Cu_{85}Zn_{15}$ and $Cu_{15}Zn_{85}$ blends after 0.5 h of milling.

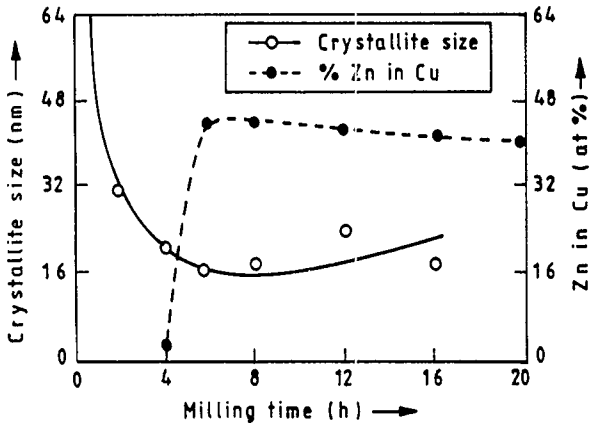

Fig. 11. Variation in the crystallite size and Zn solubility in Cu with milling time for $Cu_{50}Zn_{50}$ blend.

4. Discussion

4.1. Phase formation during MA

The stable nature of Al_3Ni in $Al_{82}Ni_{18}$ and $Al_{79}Ni_{21}$ blends that deviate from its stoichiometric composition ($Al_{75}Ni_{25}$) suggests that there could be some loss of Al owing to oxidation in course of MA thus shifting the alloy composition towards the stoichiometry of Al_3Ni. For similar reason Al_3Ni may become unstable during MA of $Al_{75}Ni_{25}$ blend. The chemical analysis of the mechanically alloyed samples reported in Table 2 has confirmed this conjecture. A similar result has been reported earlier for Al–Fe system [13] where Al_5Fe_2 (28 at.% Fe) was obtained from an elemental blend of $Al_{75}Fe_{25}$ instead of the expected Al_3Fe. However, the stability of ordered Al_3Ni in nanocrystalline powders containing 22–24 at.% Ni is quite interesting in view of the fact that Al_3Ni is a line compound under equilibrium conditions. It suggests that ordered Al_3Ni can accommodate some structural defects induced by milling. However, the stability of milled Al_3Ni seems to be more sensitive to difficiencies in the Al-sublattice, since it becomes unstable in ball milled alloys containing >25 at.% Ni.

In contrast to Al_3Ni, the stability of ordered NiAl seem to be quite insensitive to both compositional variation and structural defects induced by MA. Similar results have also been reported by other investigators [10,11]. Under ball milled condition nanocrystalline NiAl phase field could be extended more towards Al-rich side (up to 25 at.% Ni compared with equilibrium 45 at.% Ni) than towards Ni-rich side (i.e. up to 65 at.% Ni compared with 58 at.% Ni in equilibrium diagram). This is in agreement with earlier studies on conventional NiAl structure which shows more tolerance to vacancies in Ni-sublattice than Al-sublattice [23,24]. It may also be noted that the critical temperature of ordering T_C for NiAl varies in proximity of its melting point over a wide range of composition and it declines only in the vicinity of NiAl–Ni_3Al phase boundary [23]. Unlike the case of Al_3Ni or NiAl, the order parameter of Ni_3Al seems to be very sensitive to the structural defects induced by high energy ball milling and Ni_3Al was disordered even at its stoichiometric composition. It is interesting to note that even after large number of investigations in this area, there exists no report of synthesis of ordered Ni_3Al directly by MA. The low ordering energy (5 kJ mol^{-1}), low ordering temperature (638 K) [20] and the close packed nature of the crystal structure seem to be the reasons for the easy destabilisation of the order in Ni_3Al during milling. The large extension of Ni_3Al in its disorderd condition during MA (70–90 at.% Ni) in comparison with the equilibrium phase field of ordered Ni_3Al (74–76 at.% Ni) could also be related to the above reasons.

Table 2
Chemical analysis of milled powders

Composition of elemental blend (at.% Ni)	Composition of milled powder (at.% Ni)	Phases observed in XRD pattern
18	22	$Al+Al_3Ni$
21	24	Al_3Ni
25	27	NiAl

5. Mechanism of alloying

The present study on the Ni–Al system shows that ordered NiAl and Al_3Ni form suddenly after individual constituents reach some critical nanocrystalline size. The sudden exothermic reaction in the vial to yield NiAl from $Ni_{50}Al_{50}$ mixture reported by Atzmon [9] is a characteristic of reactive mixing. However, in a typical reactive mixing, the zone of reaction usually spreads in an irregular fashion. In the present case, however, it is found that crystallite size of the ordered products is the sum of the individual crystallite sizes of Ni and Al irrespective of the composition chosen. Hence, in order to distinguish this process from gradual diffusive or conventional reactive mixing, NiAl and Al_3Ni formation mechanism may be termed as discontinuous additive intermixing as indicated in Table 3. It is also conceivable that large scale and rapid intermixing of two constituents to yield an ordered product may involve a moving boundary process, once the product phase is nucleated.

In case of formation of an ordered reaction product like NiAl or Al_3Ni, the contribution of entropy change to the driving force may not be significant. Therefore, in these cases the larger the ΔH_f, the higher the driving force for the reaction. It is expected that the critical crystallite size at which such discontinuous mixing trig-

Table 3
Nature of mixing during MA

System	Phase	ΔH_f kJ mol^{-1}	Product	Mode of mixing
Cu–Zn	ϵ	7	disordered	continuous diffusive
	α	8	disordered	continuous diffusive
Ni–Al	Al_3Ni	150	ordered	discontinuous additive
	NiAl	118	ordered	discontinuous additive
	Ni_3Al	153	disordered	continuous diffusive
	(Ni(Al))	($\Delta H_{ord} \approx 5$)		

gers, should diminish with the increase in driving force. This explains why critical crystallite sizes of Al and Ni for the formation of NiAl are higher in $Al_{50}Ni_{50}$ than in $Al_{75}Ni_{25}$. It is known that the ΔH_f of NiAl is maximum at its stoichiometric composition and decreases on either side [23].

In case of Ni_3Al, the ΔH_f large (150 kJ mol^{-1}) and comparable with that for NiAl or Al_3Ni [18]. However, Ni_3Al is unable to retain its ordered structure in ball milled condition possibly due to its low ordering energy (5 kJ mol^{-1}) [19]. Since both Ni and disordered Ni_3Al are fcc, under ball milling condition Ni_3Al losses its order and distinction with the solid solution of Al in Ni. This can explain why formation of disordered Ni_3Al in Ni–Al blends containing ≥ 70 at.% Ni form by gradual enrichment of Ni with Al in a manner similar to the formation of a solid solution [15]. The absence of XRD peak shift for Al and the large peak shifts of Ni observed in course of MA suggest that Al is the major diffusing species in the formation of disordered Ni_3Al. Table 3 summarises the alloying characteristics of Ni aluminides. It is apparent that disordered phases form by continuous diffusive mixing during MA even if ΔH_f. is large

In the case of Cu–Zn system, the alloying was again observed to be by continuous diffusive mixing. This is expected, as ΔH_f of the phases in this system is quite low (8 kJ mol^{-1}) [21]. However, it is interesting to note that alloying is initiated by the diffusion of Cu into Zn, while the reverse is expected from the solubility point of view. This is not difficult to understand if one looks into the diffusivities of Cu and Zn in each other. It is clear from the simulation studies [25] and ball milling of Fe–C martensite [26] and the local rise in temperature at the point of impact on a particle in a mill is not appreciable. Assuming a temperature of about 200 °C, the diffusivities of Cu in Zn and Zn in Cu extrapolated from high temperature data are 3.0×10^{-18} and 8.2×10^{-27} m^2 s^{-1} respectively [27]. Since the diffusivity of Cu in Zn is about eight orders of magnitude higher than Zn in Cu, alloying is expected to initiate by the diffusion of Cu in Zn and the formation of Zn-rich phases such as ϵ and γ. Diffusion of Zn into Cu and formation of α phase gains momentum only after the crystallite size of Cu is brought down to few nanometers, so that the diffusion distances become small enough. Thus, it is observed from the results in Table 3, the mode of mixing is continuous diffusive, if either the ΔH_f or the ordering energy is very low for any given compound. However, the major diffusing species in either case is decided by mutual solubilities and individual intrinsic diffusivities of the components.

6. Conclusions

(1) Nanocrystalline ordered Al_3Ni, NiAl and disordered Ni_3Al have been synthesised by MA. The phase fields of the above phases have been extended to 22–25, 25–65 and 70–90 at.% Ni respectively.

(2) Stability of ordered Al_3Ni and NiAl was insensitive to structural defects while ordered Ni_3Al was not stable under present milling conditions.

(3) Nanocrystalline solid solution (α) and electron compounds such as β, γ and ϵ in Cu–Zn system could be generated by MA.

(4) The crystallite sizes are found to be dependent on the melting point and reached a minimum in the two phase field of high melting, brittle compounds.

(5) Mode of mixing is by discontinuous additive mechanism in case of ordered compounds such as Al_3Ni and NiAl. In other cases, where the ordering energy or heat of formation is very low, it follows a continuous diffusive mechanism.

Acknowledgements

The authors are grateful to the Department of Science and Technology and Aeronautical Research and Development Board, Govt. of India, for financial support.

References

[1] J.S. Benjamin, *Metall. Trans.*, *1* (1970) 2943.
[2] C.C. Koch, in R.W. Cahn (ed.), *Processing of Metals and Alloys*, VCH, New York, 1991, p. 193.
[3] B.S. Murty, *Bull. Mater. Sci.*, *16* (1993) 1.
[4] B.S. Murty, S. Ranganathan and M. Mohan Rao, *Mater. Sci. Eng.*, *A149* (1992) 231.
[5] B.S. Murty, M. Mohan Rao and S. Ranganathan, *Mater. Sci. Eng.*, (1996) in press.
[6] P.H. Shingu (ed.), Mechanical alloying, *Mater. Sci. Forum*, *88–90* (1992).
[7] A. Calka and A.P. Radlinshi, *J. Less-Common Met.*, *161* (1990) L23.

[8] E. Ivanov, T. Grigorieva, G. Gdubkova, V. Boldyrev, A.B. Fasman, S.D. Mikhailenko and O.T. Kalinina, *Mater. Lett.*, 7 (1990) 51.
[9] M. Atzmon, *Phys. Rev. Lett.*, *64* (1988) 487.
[10] T. Itsukaichi, M. Umemoto, and J.G.C. Moreno, *Scr. Metall. Mater.*, *29* (1993) 583.
[11] F. Cardellini, G. Mazzone, A. Montone and M.V. Antisari, *Acta Metall. Mater.*, *42* (1994) 2445.
[12] F. Cardellini, V. Contini, G. Mazzone and M. Vittori, *Scr. Metall. Mater.*, *28* (1993) 1035.
[13] D.K. Mukhopadhyay, C. Suryanarayana and F.H. Froes, *Scr. Metall. Mater*, *31* (1994) 333.
[14] B.S. Murty, H.S. Singh and S.K. Pabi, *Bull. Mater. Sci.*, (1996) in press.
[15] J. Zbiral, G. Jangg and G. Korb, *Mater. Sci. Forum*, *88–90* (1992) 19.
[16] Z.A. Munir, *Metall. Trans.*, *A23* (1992) 7.
[17] M. Hansen, *Constitution of Binary alloys*, McGraw Hill, New York, 1958, p. 119 and 650.
[18] O. Kubaschewski, E.L. Evans and C.B. Alcock, *Metallurgical Thermochemistry*, Pergamon, Oxford, 1967, p. 342.
[19] K. Aoki, X.M. Wang, A. Memezawa and T. Masumoto, *Mater. Sci. Eng.*, *A179/180* (1994) 390.
[20] C.C. Koch and Y.S. Cho, *Nanostructured Mater.*, *1* (1992) 207.
[21] O Kubaschewski, E.L. Evans and C.B. Alcock, *Metallurgical Thermochemistry*, Pergaman, Oxford, 1967, p. 438.
[22] A. Guinier, *X-ray Diffraction*, Freeman, San Francisco, 1963, p. 124.
[23] R.D. Noebe, R.R. Bowman and M.V. Nathal, *Int. Mater. Rev.*, *38* (1993) 193.
[24] D.B. Miracle, *Acta Metall. Mater.*, *41* (1993) 649.
[25] R.B. Schwarz and C.C. Koch, *Appl. Phys. Lett.*, *49* (1986) 146.
[26] R.M. Davis, B.T. McDermott and C.C. Koch, *Metall. Trans.*, *A19* (1988) 2867.
[27] R.C. Weast (ed.), *CRC Handbook of Chemistry and Physics*, 58th edn., CRC Press, Ohio, 1979, p. F-62.